JOURNAL OF GUIDANCE, CONTROL, AND DYNAMICS
Vol. 17, No. 5, September–October 1994

Petrov-Galerkin Finite Elements in Time for Rigid-Body Dynamics

Marco Borri* and Carlo Bottasso†
Politecnico di Milano, 20133, Milan, Italy

The problem of rigid-body rotational dynamics is examined in the context of a novel Petrov-Galerkin mixed finite-element-in-time formulation. The present approach crucially differs from other formulations in the choice of the test functions that weight the constitutive equations in an integral average sense. Within this framework, two second-order accurate time-stepping algorithms are derived: the first attains a slightly greater accuracy than the second when compared with the analytical solution of a free-tumbling rigid body with an axis of material symmetry, but in general it does not preserve energy for force-free motion; the second is marginally less accurate, but it is associated with a discrete conservation law of the kinetic energy. Numerical simulations are presented that confirm the results of the analysis and illustrate the excellent performance of the proposed numerical approach.

Nomenclature

$\mathcal{D}$	= time domain, $[0, T]$
$\mathcal{D}_i$	= time element, $[t_i, t_{i+1}]$
H	= Hamiltonian function
$\boldsymbol{H}(\cdot)$	= operator defined in Eq. (32)
$\boldsymbol{h}$	= angular momentum vector
$\boldsymbol{I}$	= 3×3 identity matrix
$\mathcal{I}_a, \mathcal{I}_t$	= axial and transverse inertia
$\boldsymbol{J}$	= spatial inertia dyadic
$\boldsymbol{k}$	= axis of rotation
$\boldsymbol{L}(\cdot, \cdot)$	= operator defined in Eq. (59)
$\boldsymbol{l}$	= linear momentum vector
$\boldsymbol{M}$	= mass
$\boldsymbol{m}$	= external torque
$(O, \boldsymbol{i}_i)$	= fixed frame of origin O, $i = 1, 2, 3$
$(P, \boldsymbol{e}_i)$	= embedded frame of origin P, $i = 1, 2, 3$
$\boldsymbol{R}(\psi)$	= rotation tensor associated with ψ
$\mathcal{R}^{-1}[\cdot]$	= inverse rotation operator
$\boldsymbol{r}$	= residual
$\boldsymbol{s}$	= external force
T	= kinetic energy
t	= time
$\boldsymbol{u}$	= linear velocity
$\boldsymbol{v}_1, \boldsymbol{v}_2$	= test functions
W_δ	= virtual work of external torque
χ	= incremental rotation, $\xi \omega \, \Delta t$
x	= position vector of P in $(O, \boldsymbol{i}_i)$, $P - Q$
α	= direction cosine matrix
$\mathcal{B}$	= rigid body
Δt	= time step, $t_{i+1} - t_i$
$\Gamma(\psi)$	= tensor defined in Eq. (4)
$\delta(\cdot)$, $\mathrm{d}(\cdot)$	= variation, increment
$\delta^\circ(\cdot)$	= corotational variation
θ_δ	= virtual rotation
ι_i, ι_{i+1}	= nodal impulses
ξ	= nondimensional coordinate in $\mathcal{D}_i$, $0 \le \xi \le 1$
ϱ	= density of $\mathcal{B}$
ψ	= rotation vector, $\psi \boldsymbol{k}$
ψ	= modulus of rotation, $\sqrt{\psi \cdot \psi}$
ω	= angular velocity
$(\cdot)$	= derivative with respect to time, $\mathrm{d}(\cdot)/\mathrm{d}t$
$(\cdot)_b$	= boundary quantity
$(\cdot)_i$	= quantity pertaining to time t_i
$(\cdot)^{(j)}$	= quantity pertaining to jth step

Received Jan 26, 1993; revision received Nov. 29, 1993; accepted for publication Nov. 29, 1993.

*Professor.

†Graduate Research Assistant; currently Post-Doctoral Research Assistant, Scientific Computation Research Center, Rensselaer Polytechnic Institute, Troy, NY 12180-3590.

Introduction

THE development of time integration schemes for rigid-body dynamics has stimulated the work of a number of authors over the years.[1–5] The interest in the solution of equations involving finite rotations is motivated by the applicability of such approaches to the exploding research area of multibody dynamics and to nonlinear structural dynamics problems, where finite element models of rods, beams, and shells result in rotational degrees of freedom described in terms of orthogonal matrices.

The problem of evolution in the orthogonal group is examined in this work in the context of a mixed Petrov-Galerkin finite-element-in-time formulation. The finite-element-in-time methodology has several distinguishing features. First, it has a physical appeal and a firm theoretical foundation, because it corresponds to a perfectly coherent impulsive view of dynamics in which forces acting on the system are transformed by the shape functions in equivalent (in an energy sense) impulses acting at discrete time instants. Moreover, for force-free motion, conservation of momentum is naturally achieved for any choice of the shape functions. This is in direct contrast with the difficulties experienced by other approaches to guarantee this fundamental conservation property.[5,6] In addition, it allows the treatment of both initial-value and boundary-value problems within the same unified framework. This unique characteristic readily allows the analysis of periodic-in-time systems and the development of linearized stability analyses about a reference configuration. This peculiarity has made the finite element in time a preferred analysis tool for rotor dynamics. Furthermore, the algorithms developed in the context of the finite-element-in-time methodology do not need to compute the acceleration, an additional computational advantage.

Starting from Hamilton's weak principle expressed in mixed form, the approach developed in this work crucially differs from other formulations in the choice of the test functions that weight the constitutive equations in an integral average sense. We propose a particular nonlinear choice of these shape functions that ensures noteworthy features to the resulting algorithms. The numerical approximation is based on a computationally convenient two-node finite element denoted by constant angular velocity and constant angular momentum within the time element, and the numerical implementation is based on an original updated Lagrangian computational procedure. Within this context, two different second-order accurate time-stepping algorithms are developed: the first, referred to as Algorithm 1 in what follows, is obtained when the integrals appearing in the weak form of the constitutive equations are evaluated analytically, whereas the second, referred to as Algorithm 2, is

obtained when the same integrals are approximated with the use of the trapezoidal rule.

The numerical characteristics of the proposed integration schemes seem to be in some way complementary: the first attains a slightly higher accuracy than classic polynomial formulations when compared with the analytical solution of a free-tumbling rigid body with an axis of material symmetry, but in general it does not preserve energy for force-free motion; the second is marginally less accurate than the first, but it is associated with a discrete conservation law of energy, which ensures unconditional stability according to the energy method.

An outline of the paper follows. We review some elementary notions related to the kinematics and dynamics of rigid bodies, in order to introduce the appropriate notation. The constitutive equations and the equations of momentum balance are discussed, together with appropriate initial conditions that complete the statement of the initial-value problem in the phase space. Then, we develop a weighted residual form that is well suited for numerical approximation, and we show that this weak form can be put in correspondence with a variational principle, namely Hamilton's weak principle. Suitable shape functions for approximating the independent fields are introduced, together with appropriate spaces for the weighting functions. The subsequent sections are devoted to the formulation and analysis of the proposed algorithms, and details are given of their linearization and step-by-step implementation. Finally, some numerical simulations are presented that illustrate the excellent numerical characteristics of the proposed time-stepping procedures and confirm the results of the analysis.

Kinematics and Dynamics of a Rigid Body

In the following, some elementary notions related to the kinematics of rigid bodies are briefly discussed in order to introduce the appropriate notation. More complete expositions can be found in classic textbooks, e.g., Refs. 7–9.

Let $(O, \boldsymbol{i}_i)$ $(i = 1, 2, 3)$ be an inertial frame of origin O and $(P, \boldsymbol{e}_i)(i = 1, 2, 3)$ a frame embedded in the rigid body $\mathcal{B}$. Particles Q of the rigid body are denoted by the distance vector $Q - P$. For convenience and without any loss of generality, we consider the origin of the embedded frame to be located in the center of mass of $\mathcal{B}$, i.e., $\int_{\mathcal{B}} \rho(Q - P)\mathrm{d}\mathcal{B} = 0$, ϱ being the density of $\mathcal{B}$.

At any time $t \in [0, T] \subset \mathcal{R}_+$, the placement of the body frame is completely identified by the position vector $\boldsymbol{x}(t) = P - O$ of its origin P with respect to the origin O of the inertial frame and by the direction cosine matrix $\alpha(t)$ according to the relation $\boldsymbol{e}_i(t) = \alpha(t) \cdot \boldsymbol{i}_i (i = 1, 2, 3)$. The term $\alpha(t)$ is an orthogonal transformation ($\alpha(t) \in \mathrm{SO}(3)\, \forall t \in [0, T]$) and hence enjoys the orthogonality property $\alpha(t) \cdot \alpha^T(t) = \boldsymbol{I}$.

Letting $\alpha(0) = \alpha_0$ be the direction cosine matrix that identifies the orientation of the embedded frame at $t = 0$, the direction cosine matrix $\alpha(t)$ at the generic time instant t is obtained by a rotation ψ of α_0 as

$$\alpha(t) = \boldsymbol{R}(\psi) \cdot \alpha_0 \tag{1}$$

$\boldsymbol{R}(\psi)$being the rotation tensor corresponding to ψ. The rotation may be conveniently expressed as $\psi = \psi \cdot \boldsymbol{k}$, ψ being the magnitude of rotation and $\boldsymbol{k}$ the rotation axis. In terms of ψ, the rotation tensor $\boldsymbol{R}$ may be expressed through the exponential map as

$$\boldsymbol{R}(\psi) = \exp(\psi \times \boldsymbol{I}) = \sum_{n=0}^{\infty} \frac{1}{n!} (\psi \times \boldsymbol{I})^n \tag{2}$$

The angular velocity ω is related to the rate of the rotation vector $\mathrm{d}\psi/\mathrm{d}t$ through the tensor Γ, which itself depends on ψ, i.e., $\omega = \Gamma(\psi) \cdot \dot{\psi}$, whereas the linear velocity simply writes $\boldsymbol{u} = \dot{\boldsymbol{x}}$. [The term $\dot{(\cdot)} = \mathrm{d}(\cdot)/\mathrm{d}t$ denotes derivative with respect to time.] The closed-form expression of the series (2) and of the tensor Γ are respectively

$$\boldsymbol{R}(\psi) = \sum_{n=0}^{\infty} \frac{1}{n!} (\psi \times \boldsymbol{I})^n = \boldsymbol{I} + a\psi \times \boldsymbol{I} + b\psi \times \psi \times \boldsymbol{I} \tag{3}$$

$$\Gamma(\psi) = \sum_{n=0}^{\infty} \frac{1}{(n+1)!} (\psi \times \boldsymbol{I})^n = \boldsymbol{I} + b\psi \times \Gamma + c\psi \times \psi \times \boldsymbol{I} \tag{4}$$

where

$$a = \frac{\sin \psi}{\psi}$$

$$b = \frac{1 - \cos \psi}{\psi^2}$$

$$c = \frac{1}{\psi^2}(1 - a)$$

The linear momentum $\boldsymbol{l}$ and the angular momentum $\boldsymbol{h}$ take the form

$$\boldsymbol{l} = \boldsymbol{M} \cdot \boldsymbol{u} \tag{5}$$

$$\boldsymbol{h} = \boldsymbol{J} \cdot \omega \tag{6}$$

Here $\boldsymbol{M} = \int_{\mathcal{B}} \varrho \, \mathrm{d}\mathcal{B}$ is the total mass of the body and $\boldsymbol{J} = -\int_{\mathcal{B}} \varrho (Q - P) \times (Q - P) \times \boldsymbol{I} \, \mathrm{d}\mathcal{B}$ is the spatial inertia dyadic. It should be remarked that, although the spatial inertia dyadic $\boldsymbol{J}$ is time variant, the convected inertia dyadic $\bar{\boldsymbol{J}} = \alpha^T \cdot \boldsymbol{J} \cdot \alpha$ is constant.

The equations of linear and angular momentum balance with respect to the center of mass are

$$\dot{\boldsymbol{l}} = \boldsymbol{s} \tag{7}$$

$$\dot{\boldsymbol{h}} = \boldsymbol{m} \tag{8}$$

$\boldsymbol{s}$ being the external force and $\boldsymbol{m}$ the external torque relative to the center of mass.

Eventually, in order to complete the statement of the initial-value problem in the phase space, we consider initial conditions of the form

$$\boldsymbol{x}(0) = \boldsymbol{x}_0 \tag{9}$$

$$\alpha(0) = \alpha_0 \tag{10}$$

and

$$\boldsymbol{u}(0) = \boldsymbol{u}_0 \tag{11}$$

$$\omega(0) = \omega_0 \tag{12}$$

In the following, we will restrict our attention to the rotational dynamic problem, governed by the constitutive equation (6), angular momentum balance equation (8), and initial conditions (10) and (12).

Weak Forms for Rigid-Body Dynamics

The constitutive equation (6) and momentum balance equation (8) can be cast in a weighted residual form that is well suited for numerical approximation. Preliminarily to the development of the weak form, consider the following partition of the time domain $\mathcal{D} = [0, T]$:

$$0 = t_1 < t_2 < \cdots < t_{n+1} = T$$

and let $\mathcal{D}_i = [t_i, t_{i+1}]$ be a typical time element, $\Delta t_i = t_{i+1} - t_i$ being the time step.

We look for a weak solution of the initial-value problem in $\mathcal{D}_i$ defined by the initial conditions $\alpha(t_i) = \alpha_i$, $\boldsymbol{h}(t_i) = \boldsymbol{h}_i$, considering the following weighted residual form:

$$\int_{t_i}^{t_{i+1}} [\boldsymbol{v}_1 \cdot (\omega - \boldsymbol{J}^{-1} \cdot \boldsymbol{h}) - \boldsymbol{v}_2 \cdot (\dot{\boldsymbol{h}} - \boldsymbol{m})] \, \mathrm{d}t = 0 \tag{13}$$

$\boldsymbol{v}_1$ being the test functions that weight the costitutive equations and $\boldsymbol{v}_2$ the test functions that weight the momentum balance equations.

Integration by parts of the term $\int_{t_i}^{t_{i+1}} \boldsymbol{v}_2 \cdot \dot{\boldsymbol{h}}\, dt$ relaxes the continuity requirements of the trial functions $\boldsymbol{h}$ and leads to

$$\int_{t_i}^{t_{i+1}} [\boldsymbol{v}_1 \cdot (\boldsymbol{\omega} - \boldsymbol{J}^{-1} \cdot \boldsymbol{h}) + \dot{\boldsymbol{v}}_2 \cdot (\boldsymbol{h} + \boldsymbol{v}_2 \cdot \boldsymbol{m})]\, dt = \boldsymbol{v}_2 \cdot \boldsymbol{h}_b \Big|_{t_i}^{t_{i+1}} \quad (14)$$

The term $(\cdot)_b$ denotes boundary quantities pertaining to the boundary time instants t_i and t_{i+1}, implying that in general $\boldsymbol{h}_{b_i}$ differs from $\boldsymbol{h}(t_i)$ and $\boldsymbol{h}_{b_{i+1}}$ differs from $\boldsymbol{h}(t_{i+1})$, as shown in Ref. 10. For a discussion on the meaning of boundary terms in weak forms for dynamics, refer to Ref. 11.

It seems interesting to remark that the weak form (14) can be put in correspondence with a variational principle. The kinetic energy T of a rigid body can be expressed in the form

$$T = \tfrac{1}{2} \boldsymbol{\omega} \cdot \boldsymbol{J} \cdot \boldsymbol{\omega} \quad (15)$$

whereas the angular momentum conjugate with $\boldsymbol{\omega}$ is $\boldsymbol{h} = \partial T / \partial \boldsymbol{\omega}$. Introducing the Hamiltonian function $H = \boldsymbol{h} \cdot \boldsymbol{\omega} - T$ associated with T and $\boldsymbol{\omega}$, the kinetic energy can be alternatively expressed as

$$T = \boldsymbol{h} \cdot \boldsymbol{\omega} - \tfrac{1}{2} \boldsymbol{h} \cdot \boldsymbol{J}^{-1} \cdot \boldsymbol{h} \quad (16)$$

Consider a configuration of the rigid body $\mathcal{B}$ identified by the direction cosine matrix α. Consider now a varied configuration, denoted by $\delta\alpha = \theta_\delta \times \alpha$, θ_δ being the virtual variation that brings α in $\delta\alpha$. (In this work, the notation θ_δ has been preferred to that of $\delta\theta$ to signify that θ_δ cannot be interpreted as the variation of true coordinates.) Variation of the kinetic energy expressed in Eq. (16) is written

$$\delta T = \delta^\circ \boldsymbol{h} \cdot (\boldsymbol{\omega} - \boldsymbol{J}^{-1} \cdot \boldsymbol{h}) + \delta^\circ \boldsymbol{\omega} \cdot \boldsymbol{h} \quad (17)$$

The term $\delta^\circ(\cdot)$ denotes corotational variation, which reads for a vector $\delta^\circ(\cdot) = \alpha \cdot \delta[\alpha^T(\cdot)]$ and it is consequently related to the variation $\delta(\cdot)$ through the expression

$$\delta(\cdot) = \delta^\circ(\cdot) + \theta_\delta \times (\cdot) \quad (18)$$

The corotational variation is defined for a second-order tensor as $\delta^\circ(\cdot) = \alpha \cdot \delta(\alpha^T \cdot (\cdot) \cdot \alpha) \cdot \alpha^T$. The corotational variation can be interpreted as a three-step procedure: first, the quantity to be varied is pulled back along the flow, then the variation is taken, and eventually the result is pushed forward to the current position. It is immediate to prove that the corotational variation of the angular velocity coincides with the absolute time derivative of the virtual rotation, i.e.,

$$\delta^\circ \boldsymbol{\omega} = \delta\boldsymbol{\omega} - \theta_\delta \times \boldsymbol{\omega} = \frac{d}{dt} \theta_\delta \quad (19)$$

The virtual work W_δ of the external torques $\boldsymbol{m}$ is then

$$W_\delta = \theta_\delta \cdot \boldsymbol{m} \quad (20)$$

(The notation W_δ is preferred here to δW, emphasizing that W_δ is not in general a virtual change of any functional W.)

It appears clear at this point that, interpreting the test functions $\boldsymbol{v}_1$ and $\boldsymbol{v}_2$ as $\boldsymbol{v}_1 = \delta^\circ \boldsymbol{h}$ and $\boldsymbol{v}_2 = \theta_\delta$, one gets, from Eq. (14), the following weak form:

$$\int_{t_i}^{t_{i+1}} [\delta^\circ \boldsymbol{h} \cdot (\boldsymbol{\omega} - \boldsymbol{J}^{-1} \cdot \boldsymbol{h}) + \delta^\circ \boldsymbol{\omega} \cdot \boldsymbol{h} + \theta_\delta \cdot \boldsymbol{m}]\, dt = \theta_\delta \cdot \boldsymbol{h}_b \Big|_{t_i}^{t_{i+1}} \quad (21)$$

which corresponds to the well-known Hamilton weak principle

$$\int_{t_i}^{t_{i+1}} (\delta T + W_\delta)\, dt = \theta_\delta \cdot \boldsymbol{h}_b \Big|_{t_i}^{t_{i+1}} \quad (22)$$

The form expressed in Eq. (21) is a mixed form, in the sense that rotations and momenta represent two independent fields and the constitutive relation $\boldsymbol{h} = \boldsymbol{J} \cdot \boldsymbol{\omega}$ is only weakly enforced.

Introducing suitable shape functions for approximating the independent fields and selecting appropriate spaces for the weighting functions, this form provides the basis for developing effective integration algorithms for rigid-body dynamics.[4] This crucial point will be the topic addressed in the next section.

Finite Element Approximation

In this section we propose simple but effective choices of the test and trial functions appearing in the governing weak form (21), which provide remarkable numerical properties to the resulting integration algorithms. The numerical implementation is based on an updated Lagrangian procedure, in the sense that rotations of the rigid body $\mathcal{B}$ in $\mathcal{D}_i$ are measured from the orientation defined by the direction cosine matrix $\alpha(t_i) = \alpha_i$. Then, the direction cosine matrix at the generic time instant $t \in \mathcal{D}_i$ is given by

$$\alpha(t) = \boldsymbol{R}(\chi) \cdot \alpha_i \quad (23)$$

χ being the incremental rotation that brings α_i in α.

We consider a constant angular velocity within the time interval; hence the rotation χ is parallel to $\boldsymbol{\omega}$ and can be expressed as the linear function $\chi = \xi \boldsymbol{\omega}\, \Delta t$, ξ being a nondimensional coordinate in $\mathcal{D}_i$ ($0 \le \xi \le 1$). Analogously, we consider a constant angular momentum $\boldsymbol{h}$ within $\mathcal{D}_i$.

The interpolation of the virtual rotation θ_δ needed for evaluating the contribution to virtual work of the external torques is selected to be the following linear interpolation of the nodal values θ_{δ_i} and $\theta_{\delta_{i+1}}$:

$$\theta_\delta = (1 - \xi)\theta_{\delta_i} + \xi \theta_{\delta_{i+1}} \quad (24)$$

So far, this is the classic polynomial interpolation of the independent fields for a two-node element, as used, e.g., in Ref. 3. We depart from this standard approach in the selection of the test functions $\delta^\circ \boldsymbol{h}$ that weight the costitutive equation in an integral average sense. In the spirit of a Petrov-Galerkin approximation, we propose, in this work, a nonlinear interpolation of $\delta^\circ \boldsymbol{h}$, expressed as

$$\delta^\circ \boldsymbol{h} = \boldsymbol{R}(\chi) \cdot \boldsymbol{h}_\delta \quad (25)$$

$\boldsymbol{h}_\delta$ being a constant nodal value.

With this choice of test and trial functions, the discrete equations of motion resulting from the weak form (21) are written as

$$\boldsymbol{h} = \boldsymbol{h}_{b_i} + \iota_i \quad (26)$$

$$\boldsymbol{h}_{b_{i+1}} = \boldsymbol{h} + \iota_{i+1} \quad (27)$$

$$\boldsymbol{\omega} = \boldsymbol{J}_i^{-1} \cdot \boldsymbol{H}(\boldsymbol{\omega}\, \Delta t) \cdot \boldsymbol{h} \quad (28)$$

$$\alpha_{i+1} = \boldsymbol{R}(\boldsymbol{\omega}\, \Delta t) \cdot \alpha_i \quad (29)$$

$\boldsymbol{J}_i$ being the spatial inertial dyadic at time t_i and

$$\iota_i = \int_0^1 (1 - \xi) \boldsymbol{m}\, \Delta t\, d\xi \quad (30)$$

$$\iota_{i+1} = \int_0^1 \xi \boldsymbol{m}\, \Delta t\, d\xi \quad (31)$$

are the impulses acting at time nodes t_i and t_{i+1}, respectively. One can use a linear interpolation of $\boldsymbol{m}$ for the evaluation of ι_i and ι_{i+1}, setting $\boldsymbol{m}(\xi) = (1 - \xi)\boldsymbol{m}(t_i) + \xi \boldsymbol{m}(t_{i+1})$. In Eq. (28),

$$\boldsymbol{H}(\boldsymbol{\omega}\, \Delta t) = \int_0^1 \boldsymbol{R}^T(\chi)\, d\xi \quad (32)$$

is understood.

We make the following remarks:

1) In the absence of external torque, the discrete algorithmic problem defined by Eqs. (26–29) guarantees the conservation of angular momentum. To prove this conservation property, set $\boldsymbol{m} = 0$ in $\mathcal{D}_i$, and hence $\iota_i = \iota_{i+1} = 0$. Then, from Eqs. (26) and (27) it is immediately obtained that momenta are continuous at the element boudaries, according to the expression $\boldsymbol{h}_{b_i} = \boldsymbol{h} = \boldsymbol{h}_{b_{i+1}}$.

2) The discrete equations of motion (26–29) correspond to a consistent impulsive view of dynamics. If a forcing function is acting on the system, it is weighted by the shape functions and it is transformed through relations (30) and (31) in equivalent (in an energy sense) impulses at the time nodes t_i and t_{i+1}. The first impulse ι_i causes

a jump discontinuity at time t_i that transforms the initial angular momentum $\boldsymbol{h}_{b_i}$ in $\boldsymbol{h}$, according to Eq. (26). Then the body travels in torque-free motion at constant angular momentum until time t_{i+1}, when the second impulse ι_{i+1} causes a second jump discontinuity from $\boldsymbol{h}$ to $\boldsymbol{h}_{b_{i+1}}$, as shown by Eq. (27).

3) When the external torques are configuration independent, the discrete momentum balance equations (26) and (27), linear in the unknown momenta $\boldsymbol{h}$ and $\boldsymbol{h}_{b_{i+1}}$, are fully decoupled from Eq. (28).

In the following, two algorithms are proposed that differ in the evaluation of the integral $\boldsymbol{H}(\omega\,\Delta t)$.

Algorithm 1

The first algorithm is based on the exact evaluation of the integral $\boldsymbol{H}(\omega\,\Delta t) = \int_0^1 \boldsymbol{R}^T(\chi)\,\mathrm{d}\xi$. From the expressions of the tensors $\boldsymbol{R}$ and Γ, it is immediate to prove that

$$\int_0^1 \boldsymbol{R}(\chi)\,\mathrm{d}\xi = \Gamma(\omega\,\Delta t) \tag{33}$$

Then, the algorithmic problem is defined in $\mathcal{D}_i$ by the following set of discrete equations:

$$\boldsymbol{h} = \boldsymbol{h}_{b_i} + \iota_i \tag{34}$$

$$\boldsymbol{h}_{b_{i+1}} = \boldsymbol{h} + \iota_{i+1} \tag{35}$$

$$\omega = \boldsymbol{J}_i^{-1} \cdot \Gamma^T(\omega\,\Delta t) \cdot \boldsymbol{h} \tag{36}$$

$$\alpha_{i+1} = \boldsymbol{R}(\omega\,\Delta t) \cdot \alpha_i \tag{37}$$

where the initial data α_i and $\boldsymbol{h}_{b_i}$ at time t_i are known.

We remark the following:

1) As previously shown, this algorithm conserves the angular momentum for torque-free motion, but in general it does not preserve the kinetic energy.

2) The algorithm is convergent and second order accurate. A numerical check of this assertion will be given in the following.

3) Equation (36) is nonlinear in ω, and hence a consistent linearization is needed for numerical implementation in order to resort to a Newton-Raphson–like iterative procedure.

Algorithm 2

The second algorithm is based on the approximate solution of the integral $\boldsymbol{H}(\omega\,\Delta t) = \int_0^1 \boldsymbol{R}^T(\chi)\mathrm{d}\xi$ using the trapezoidal rule, which gives

$$\boldsymbol{H}(\omega\,\Delta t) \approx \tfrac{1}{2}[\boldsymbol{R}^T(\omega\,\Delta t) + \boldsymbol{I}] \tag{38}$$

The algorithmic problem in $\mathcal{D}_i$ is defined by the following set of discrete equations:

$$\boldsymbol{h} = \boldsymbol{h}_{b_i} + \iota_i \tag{39}$$

$$\boldsymbol{h}_{b_{i+1}} = \boldsymbol{h} + \iota_{i+1} \tag{40}$$

$$\omega = \tfrac{1}{2}\boldsymbol{J}_i^{-1} \cdot [\boldsymbol{R}^T(\omega\Delta t) + \boldsymbol{I}] \cdot \boldsymbol{h} \tag{41}$$

$$\alpha_{i+1} = \boldsymbol{R}(\omega\,\Delta t) \cdot \alpha_i \tag{42}$$

where the initial data α_i and $\boldsymbol{h}_{b_i}$ are given.

All the remarks made for Algorithm 1 are valid even in this case, except that Algorithm 2 preserves energy for torque-free motion. In order to see this, let the applied torque in $\mathcal{D}_i$ be $\boldsymbol{m} = 0$. Preliminary to the proof of the energy conservation property, define, for convenience,

$$\hat{\omega}_i = \boldsymbol{J}_i^{-1} \cdot \boldsymbol{h}$$

$$\hat{\omega}_{i+1} = \boldsymbol{J}_{i+1}^{-1} \cdot \boldsymbol{h}$$

and recall that $\det(\boldsymbol{R} - \boldsymbol{I}) = 0$, i.e., the rotation tensor has one real unit eigenvalue, whose corresponding eigenvector is the axis of rotation. Hence $\omega - \boldsymbol{R}(\omega\Delta t) \cdot \omega = 0$, and from Eq. (41) we get

$$\begin{aligned} 2[\omega - \boldsymbol{R}(\omega\,\Delta t) \cdot \omega] &= \left[\boldsymbol{J}_i^{-1} \cdot (\boldsymbol{R}^T(\omega\,\Delta t) + \boldsymbol{I}\right] \\ &\quad - \boldsymbol{R}(\omega\,\Delta t) \cdot \boldsymbol{J}_i^{-1} \cdot \left[\boldsymbol{R}^T(\omega\,\Delta t) + \boldsymbol{I})\right] \cdot \boldsymbol{h} \\ &= \boldsymbol{R}^T(\omega\,\Delta t) \cdot \hat{\omega}_{i+1} + \hat{\omega}_i - \hat{\omega}_{i+1} - \boldsymbol{R}(\omega\,\Delta t) \cdot \hat{\omega}_i \\ &= 0 \end{aligned} \tag{43}$$

and consequently

$$\begin{aligned} \hat{\omega}_i - \hat{\omega}_{i+1} &= \boldsymbol{R}(\omega\,\Delta t) \cdot \hat{\omega}_i - \boldsymbol{R}^T(\omega\,\Delta t) \cdot \hat{\omega}_{i+1} \\ &= \left[\boldsymbol{R}(\omega\,\Delta t) \cdot \boldsymbol{J}_i^{-1} - \boldsymbol{J}_i^{-1} \cdot \boldsymbol{R}^T(\omega\,\Delta t)\right] \cdot \boldsymbol{h} \end{aligned} \tag{44}$$

With this expression at hand, we are now in a position to prove the conservation of energy. The kinetic energy jump in $\mathcal{D}_i$ may be written as

$$2(T_i - T_{i+1}) = \boldsymbol{h}_{b_i} \cdot \boldsymbol{J}_i^{-1} \cdot \boldsymbol{h}_{b_i} - \boldsymbol{h}_{b_{i+1}} \cdot \boldsymbol{J}_{i+1}^{-1} \cdot \boldsymbol{h}_{b_{i+1}} \tag{45}$$

which can be expressed, recalling the angular momentum conservation property, as

$$2(T_i - T_{i+1}) = \boldsymbol{h} \cdot (\hat{\omega}_i - \hat{\omega}_{i+1}) \tag{46}$$

From Eqs. (44) and (46), the discrete conservation law

$$2(T_i - T_{i+1}) = \boldsymbol{h} \cdot \boldsymbol{R}(\omega\,\Delta t) \cdot \boldsymbol{J}_i^{-1} \cdot \boldsymbol{h} - \boldsymbol{h} \cdot \boldsymbol{J}_i^{-1} \cdot \boldsymbol{R}^T(\omega\,\Delta t) \cdot \boldsymbol{h} \equiv 0 \tag{47}$$

immediately follows. This result implies unconditional stability according to the energy method.

Linearization of Algorithms

The discrete constitutive equation (28) is clearly a nonlinear function of the angular velocity ω. Therefore, a consistent linearization of the algorithmic problem is needed for numerical implementation in order to resort to a Newton-Raphson–like iterative solution strategy.

Consider first the linearization of the discrete momentum balance equation (26), which is straightforward and is written as

$$\boldsymbol{h} + \mathrm{d}\boldsymbol{h} = \boldsymbol{h}_{b_i} + \iota_i + \mathrm{d}\iota_i \tag{48}$$

where

$$\mathrm{d}\iota_i = \int_0^1 (1 - \xi)\,\mathrm{d}\boldsymbol{m}\,\Delta t\,\mathrm{d}\xi$$

Clearly, the term $\mathrm{d}\boldsymbol{m}$ cannot be specified further without any knowledge of the nature of the external torques. We remark that Eq. (27) can be used for recovering the boundary momentum $\boldsymbol{h}_{b_{i+1}}$ once at convergence and hence need not to be linearized.

Consider now the linearization of the discrete constitutive equation (28). To this aim, we develop the expression of the virtual variation of the constant angular velocity in $\mathcal{D}_i$, which can be put in relation with its infinitesimal increment expressed in terms of the incremental rotations at the boundary nodes i and $i + 1$. We recall that the direction cosine matrix at the generic time instant $t \in \mathcal{D}_i$ is given by

$$\alpha(t) = \boldsymbol{R}(\chi) \cdot \alpha_i \tag{49}$$

and hence

$$\delta\alpha = \delta\boldsymbol{R}(\chi) \cdot \alpha_i + \boldsymbol{R}(\chi) \cdot \delta\alpha_i \tag{50}$$

or, alternatively, by definition

$$\delta\alpha = \theta_\delta \times \alpha \tag{51}$$

Taking advantage on the fact that

$$\chi_\delta \times \boldsymbol{I} = \delta\boldsymbol{R}(\chi) \cdot \boldsymbol{R}^T(\chi) \tag{52}$$

and that the virtual rotation χ_δ is related to the virtual change of the rotation vector $\delta\chi$ through the relation

$$\chi_\delta = \Gamma(\chi)\cdot\delta\chi \tag{53}$$

one gets, from Eqs. (50) and (51),

$$\theta_\delta = \Gamma(\chi)\cdot\delta\chi + \boldsymbol{R}(\chi)\cdot\theta_{\delta_i} \tag{54}$$

Evaluating Eq. (54) at time t_{i+1}, one immediately gets the expression of the virtual variation of the angular velocity as

$$\delta\omega = \frac{1}{\Delta t}\Gamma^{-1}(\omega\,\Delta t)\cdot\theta_{\delta_{i+1}} - \frac{1}{\Delta t}\Gamma^{-T}(\omega\,\Delta t)\cdot\theta_{\delta_i} \tag{55}$$

where it has been made use of the property

$$\boldsymbol{R} = \Gamma^{-T}\cdot\Gamma = \Gamma\cdot\Gamma^{-T} \tag{56}$$

From expression (55), the increment of angular velocity $\mathrm{d}\omega$ for an initial-value problem is written as

$$\mathrm{d}\omega = \frac{1}{\Delta t}\Gamma^{-1}(\omega\,\Delta t)\cdot\theta_{\mathrm{d}_{i+1}} \tag{57}$$

$\theta_{\mathrm{d}_{i+1}}$ being the incremental rotation at time node $i+1$. (For an initial-value problem, α_i is given. This implies $\theta_{\mathrm{d}_i} \equiv 0$.)

With this result at hand, the linearization of Eq. (28) is simply written as

$$\left[\boldsymbol{I} - \boldsymbol{J}_i^{-1}\cdot\boldsymbol{L}(\omega\,\Delta t, \boldsymbol{h})\Delta t\right]\cdot\Gamma^{-1}(\omega\,\Delta t)\cdot\theta_{\mathrm{d}_{i+1}}$$
$$= -\Delta t\left[\omega - \boldsymbol{J}_i^{-1}\cdot\boldsymbol{H}(\omega\,\Delta t)\cdot(\boldsymbol{h}+\mathrm{d}\boldsymbol{h})\right] \tag{58}$$

$\boldsymbol{L}(\psi, \boldsymbol{v})$ being the directional derivative of $\boldsymbol{H}(\psi)$ applied to the generic vector $\boldsymbol{v}$, i.e.,

$$\mathrm{d}\boldsymbol{H}(\psi)\cdot\boldsymbol{v} = \boldsymbol{L}(\psi, \boldsymbol{v})\cdot\mathrm{d}\psi \tag{59}$$

Step-by-Step Implementation of Algorithms

Details of the step-by-step implementation of the proposed algorithms are given in the following. For simplicity, we do not consider the linearization of the configuration-dependent external torques.

1) Data available from converged solution at time step $i-1$: angular momentum $\boldsymbol{h}_{b_i}$, direction cosine matrix α_i, and additional data—inverse of spatial inertia dyadic $\boldsymbol{J}_i^{-1}$.

2) Prediction phase: Predict direction cosine matrix α_{i+1} at time t_{i+1} at constant angular velocity: Evaluate angular velocity at time t_i ($\omega_{b_i} = \boldsymbol{J}_i^{-1}\cdot\boldsymbol{h}_{b_i}$) and perform prediction $[\alpha_{i+1}^{(1)} = \boldsymbol{R}(\omega_{b_i}\Delta t)\cdot\alpha_i]$.

3) Iteratively solve linearized discrete equations of motion:

i) Until error $\varepsilon \le$ tolerance, do steps 1–9:

1) increment iteration counter, $j \leftarrow j+1$;

2) $\boldsymbol{R}(\omega^{(j)}\Delta t) = \alpha_{i+1}^{(j)}\cdot\alpha_i^T$;

3) compute angular velocity, $\omega^{(j)}\,\Delta t = \mathcal{R}^{-1}[\boldsymbol{R}\,(\omega^{(j)}\Delta t)]$

4) evaluate nodal impulse at time t_i, $\iota_i^{(j)} = \frac{1}{3}\,\Delta t\,\boldsymbol{m}(t_i) + \frac{1}{6}\,\Delta t\,\boldsymbol{m}^{(j)}\,(t_{i+1})$;

5) compute internal angular momentum, $\boldsymbol{h}^{(j)} = \boldsymbol{h}_{b_i} + \iota_i^{(j)}$;

6) compute residual, $\boldsymbol{r}^{(j)} = \omega^{(j)}\,\Delta t - \boldsymbol{J}_i^{-1}\cdot\boldsymbol{H}(\omega^{(j)}\,\Delta t)\cdot\boldsymbol{h}^{(j)}\,\Delta t$;

7) evaluate error, $\varepsilon = \|\boldsymbol{r}^{(j)}\|$;

8) compute incremental rotation at time t_{i+1}, $\theta_{\mathrm{d}_{i+1}}^{(j)} = -\Gamma\,(\omega^{(j)}\,\Delta t)\cdot[\boldsymbol{I} - \boldsymbol{J}_i^{-1}\cdot\boldsymbol{L}\,(\omega^{(j)}\,\Delta t, \boldsymbol{h}^{(j-1)})\,\Delta t]^{-1}\cdot\boldsymbol{r}^{(j)}$; and

9) update direction cosine matrix at time t_{i+1}, $\alpha_{i+1}^{(j+1)} = \boldsymbol{R}\,(\theta_{\mathrm{d}_{i+1}}^{(j)})\cdot\alpha_{i+1}^{(j)}$.

ii) Evaluate nodal impulse at time t_{i+1}: $\iota_{i+1} = \frac{1}{6}\,\Delta t\,\boldsymbol{m}(t_i) + \frac{1}{3}\,\Delta t\,\boldsymbol{m}(t_{i+1})$.

iii) Recover boundary angular momentum: $\boldsymbol{h}_{b_{i+1}} = \boldsymbol{h}^{(j)} + \iota_{i+1}$.

iv) Update inverse of spatial inertia dyadic: $\boldsymbol{J}_{i+1}^{-1} = \boldsymbol{R}(\omega^{(j)}\,\Delta t)\cdot\boldsymbol{J}_i^{-1}\cdot\boldsymbol{R}^T\,(\omega^{(j)}\,\Delta t)$.

4) Begin new time step.

At step 8 of the iterative Newton-Raphson procedure, one can use the approximate form $\theta_{\mathrm{d}_{i+1}}^{(j)} = -\Gamma(\omega^{(j)}\Delta t)\cdot\boldsymbol{r}^{(j)}$ in order to compute the incremental rotation at time t_{i+1} if the term $\boldsymbol{J}_i^{-1}\cdot\boldsymbol{L}(\omega^{(j)}\Delta t, \boldsymbol{h}^{(j-1)})\Delta t$ is small when compared to $\boldsymbol{I}$.

We remark that periodic-in-time problems can be readily treated within this context: assuming a period of time $\mathcal{T} = [t_1, t_2]$ and assembling a suitable number of time elements in $\mathcal{T}$, the solution is simply obtained by enforcing the appropriate periodicity conditions $\alpha_1 = \alpha_2$ and $\boldsymbol{h}_{b_1} = \boldsymbol{h}_{b_2}$.

Numerical Studies

This section focuses on the evaluation of the numerical performance of the two algorithms developed in this work. Two relevant example problems are addressed: the first deals with the force-free tumbling of a rigid body with an axis of material symmetry, and it is used for evaluating the accuracy of the algorithms as well as showing their convergence rates; the second is concerned with the unstable motion about the axis of intermediate moment of inertia, and it is here addressed to show the discrete conservation properties of the algorithms.

Torque-Free Rigid Body with Axis of Material Symmetry

This problem represents a very convenient benchmark for every formulation for rigid-body dynamics, since the analytical solution is well known.

The problem statement for the free-tumbling body is the same as that of Ref. 3: the ratio of transverse to axial inertia is $\mathcal{J}_t/\mathcal{J}_\alpha = 1.875$, the angular velocity is 15 rad/s about the axis of symmetry and 10 rad/s about the transverse axis, and the time step length $\Delta t = 0.015$ s. Three different integration schemes have been considered: Algorithms 1 and 2 developed in the preceding sections and a two-node mixed finite element in time developed in Ref. 3. Besides the updated Lagrangian implementation, this latter finite element crucially differs from the ones cosidered in this work in the choice of the test functions $\delta^\circ\boldsymbol{h}$, which are selected as constant functions in $\mathcal{D}_i$. This algorithm preserves the angular momentum $\boldsymbol{h}$ in case of torque-free motion but in general does not conserve energy.

The results are shown in Fig. 1 for a total integration time of 6 s, corresponding to a global rotation ψ_f of roughly 100 rad. The results plotted are in terms of the normalized magnitude of the difference of rotation between the calculated and the closed-form solutions, noted $\|e\|/\psi_f$. On the basis of the results reported in Fig. 1, we make the following remarks:

1) Algorithm 1 is highly accurate and its error is less than that generated by the algorithm discussed in Ref. 3.

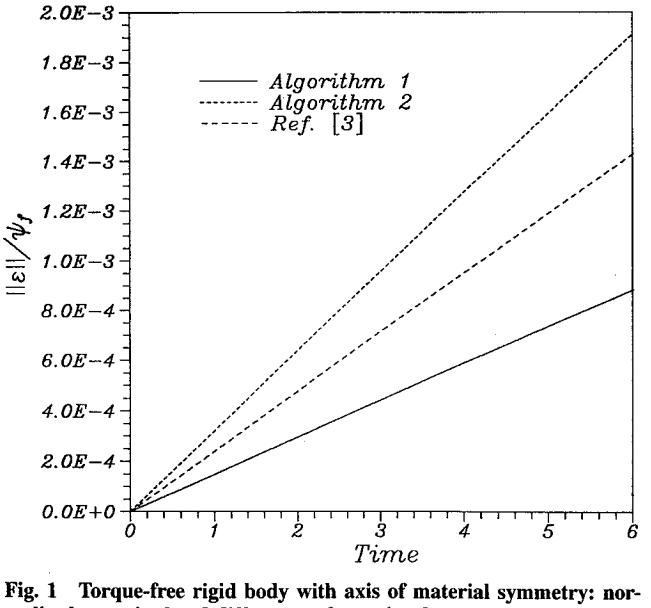

Fig. 1 Torque-free rigid body with axis of material symmetry: normalized magnitude of difference of rotation between calculated and closed-form solutions (Algorithms 1 and 2 and Ref. 3).

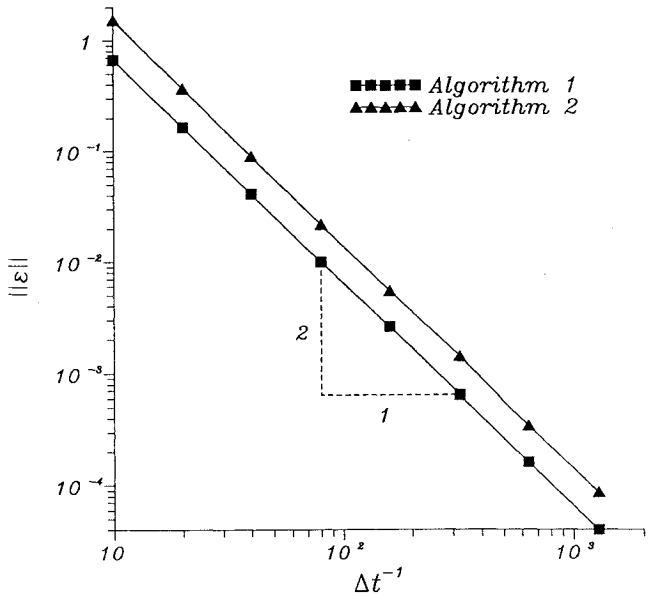

Fig. 2 Torque-free rigid body with axis of material symmetry: convergence rates of Algorithms 1 and 2.

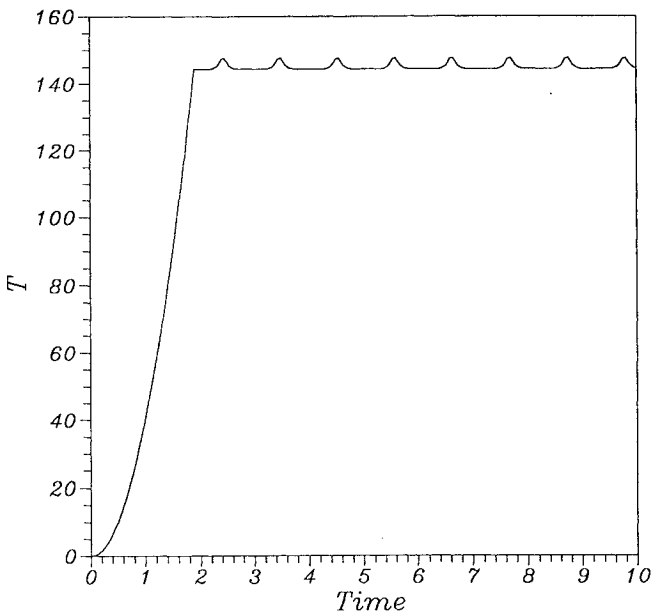

Fig. 3 Unstable rotation about axis of intermediate moment of inertia: kinetic energy (Algorithm 1).

2) The conservation of energy in Algorithm 2 is achieved at the cost of a decreased accuracy. This result raises an interesting question: given the same computational effort, is it much more desirable to guarantee the conservation of energy or to attain a higher level of accuracy in the evaluation of the state variables? In the authors' opinion, although conservation properties lead to rigorous notions of nonlinear stability, the question remains open.

Figure 2 compares the convergence rates of Algorithms 1 and 2, reporting in log-log plot the error $\|\varepsilon\|$ after 1 s of integration as a function of Δt^{-1}. It appears clear that, although Algorithm 1 is slightly more accurate than Algorithm 2, both integration schemes attain second-order accuracy.

Unstable Rotation About Axis of Intermediate Moment of Inertia

This problem is concerned with the numerical simulation of the unstable motion of a rigid body about its axis of intermediate inertia, and it is taken from Ref. 5. The problem statement is the following:

1) A constant torque about the axis of intermediate inertia is applied to a rigid body initially at rest.

2) At time $t = \bar{t}$, the constant torque is removed and a constant disturbance torque is applied to the body for a duration Δt. The disturbance torque acts about a direction normal to the initial torque.

3) Then, the body undergoes a torque-free motion.

The time history of the external torque is the following:

$$\boldsymbol{m}(t) = \begin{cases} a_1 \boldsymbol{i}_1, & 0 \le t \le \bar{t} \\ a_2 \boldsymbol{i}_2, & \bar{t} \le t \le \bar{t} + \Delta t \\ 0, & t > \bar{t} + \Delta t \end{cases}$$

where $a_1 = 20, a_2 = 0.2/\Delta t$, and $\bar{t} = 2 - \Delta t$. The convected inertia dyadic considered in this simulation is $\bar{\boldsymbol{J}} = \text{diag}(5, 10, 1)$ and the time step length is $\Delta t = 0.05$.

Figures 3–6 show the results obtained in terms of time histories of kinetic energy, angular momentum, and norm of the incremental rotation.

Figures 3 and 4 confirm our proof of the conservation of energy of Algorithm 2 for the torque-free motion corresponding to $t > 2$. Note that, as previously claimed, Algorithm 1 does not conserve energy, as shown by the ripples appearing in the time history of the kinetic energy. Threse ripples diminish in amplitude when decreasing the time step length and essentially vanish for an integration time iterval $\Delta t = 0.01$.

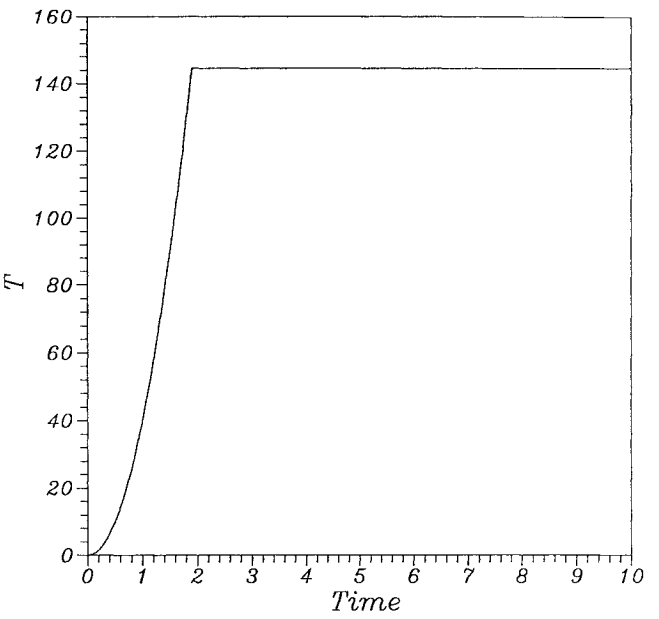

Fig. 4 Unstable rotation about axis of intermediate moment of inertia: kinetic energy (Algorithm 2).

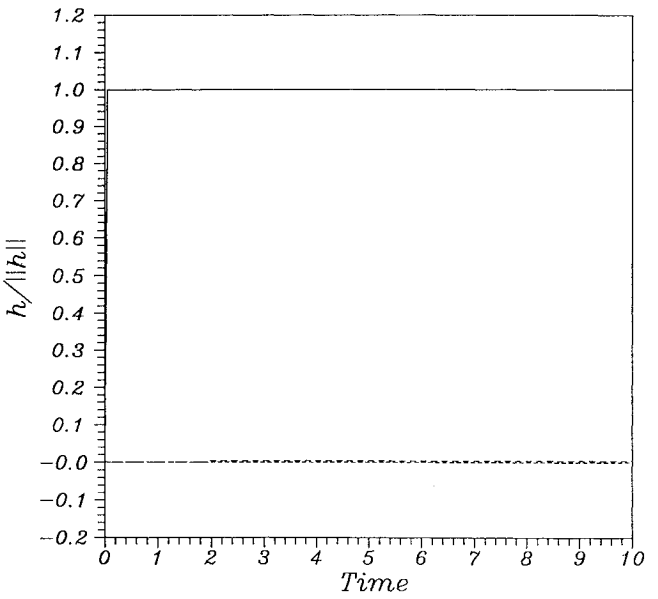

Fig. 5 Unstable rotation about axis of intermediate moment of inertia: angular momenta (Algorithm 1).

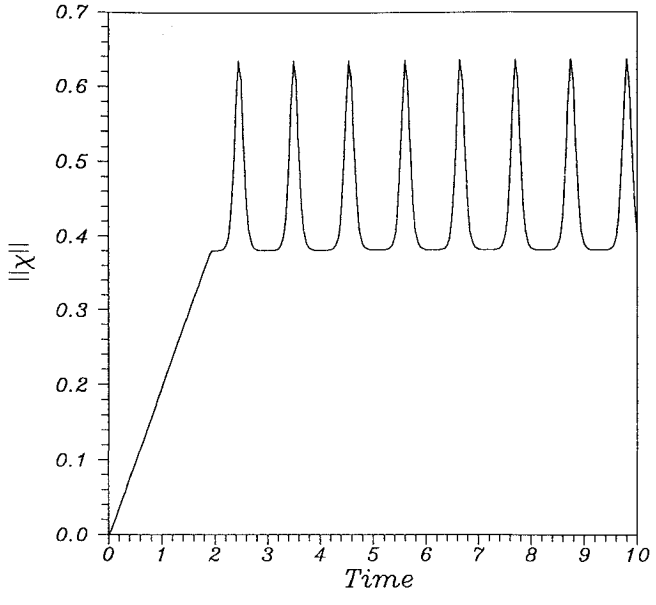

Fig. 6 Unstable rotation about axis of intermediate moment of inertia: norm of incremental rotation (Algorithm 1).

Figures 5 and 6 have been obtained using Algorithm 1, but very similar results can be produced using Algorithm 2. Figure 5 shows from a numerical point of view the previously proved conservation of angular momentum.

Figure 6 depicts the time history of the norm of the incremental rotation, $\|\chi\|$. The highly oscillating nature of the plot suggests that the use of a time step length control strategy is an important potential area for future research efforts.

Conclusions

The problem of rigid-body rotational dynamics has been considered in the context of a novel Petrov-Galerkin mixed finite-element-in-time formulation, which readily allows the treatment of initial- and boundary-value problems. This approach has a physical appeal, in that it corresponds to an impulsive view of dynamics.

Within this framework, two different second-order accurate algorithms have been developed: the first does not in general guarantee the conservation of energy for force-free motion; the second is unconditionally stable according to the energy method, and it is marginally less accurate than the former when compared with the analytical solution.

Details of the linearization and of the step-by-step implementation have been given and thoroughly discussed. The interesting performance of the proposed algorithms has been demonstrated in a number of representative simulations that confirm the results of the analysis.

References

[1]Geradin, M., and Cardona, A., "Kinematics and Dynamics of Rigid and Flexible Mechanisms Using Finite Element and Quaternion Algebra," *Comp. Mech.*, Vol. 4, 1989, pp. 115–135.

[2]Iura, M., and Atluri, S. N., "On a Consistent Theory and Variational Formulation of Finitely Stretched and Rotated 3-D Space Curved Beams," *Comp. Mech.*, Vol. 4, 1989, pp. 73–88.

[3]Mello, F. J., "Weak Formulations in Analytical Dynamics, with Applications to Multi-Rigid-Body Systems, Using Time Finite Elements," Ph.D. Dissertation, Georgia Institute of Technology, Atlanta, GA, 1989.

[4]Borri, M., Mello, F. J., and Atluri, S. N., "Variational Approaches for Dynamics and Time Finite Elements: Numerical Studies," *Comp. Mech.*, Vol. 7, 1991, pp. 49–76.

[5]Simo, J. C., and Wong, K. K., "Unconditionally S0163 Algorithms for Rigid Body Dynamics That Exactly Preserve Energy and Momentum," *Int. J. Num. Meth. Eng.*, Vol. 31, 1991, pp. 19–52.

[6]Simo, J. C., and Vu-Quoc, L., "On the Dynamics in Space of Rods Undergoing Large Motions—A Geometrically Exact Approach," *Comp. Meth. Appl. Mech. Eng.*, Vol. 66, 1988, pp. 125–161.

[7]Levi-Civita, T., and Amaldi, U., *Lezioni di Meccanica Razionale*, Zanichelli, Bologna, Italy, 1926.

[8]Arnold, V. I., *Mathematical Methods of Classical Mechanics*, Springer-Verlag, Berlin, 1978.

[9]Wittaker, E. T., *A Treatise on Analytical Dynamics*, Dover, New York, 1986.

[10]Borri, M., Ghiringhelli, G. L., Lanz, M., Mantegazza, P., and Merlini, T., "Dynamic Response of Mechanical Systems by a Weak Hamiltonian Formulation," *Comp. & Struct.*, Vol. 20, 1985, pp. 495–508.

[11]Borri, M., and Bottasso, C., "A General Framework for Interpreting Time Finite Element for Dynamics," *Comp. Mech.* (to be published).

[12]Richmayer, R. D., and Morton, K. W., *Difference Methods for Initial Value Problems*, 2nd ed., Interscience, New York, 1967.